Supplemental Information

Arc oligomerization is regulated by CaMKII phosphorylation of GAG domain; an essential mechanism for plasticity and memory formation.

Wenchi Zhang, Yang-An Chuang, Youn Na, Zengyou Ye, Liuqing Yang, Raozhou Lin, Jiechao Zhou, Jing Wu, Alena Savonenko, Daniel J. Leahy, Richard Huganir, David J. Linden, Paul F. Worley

Inventory of Supplemental Information

Supplemental Figures, Figure Legends

Figure S1

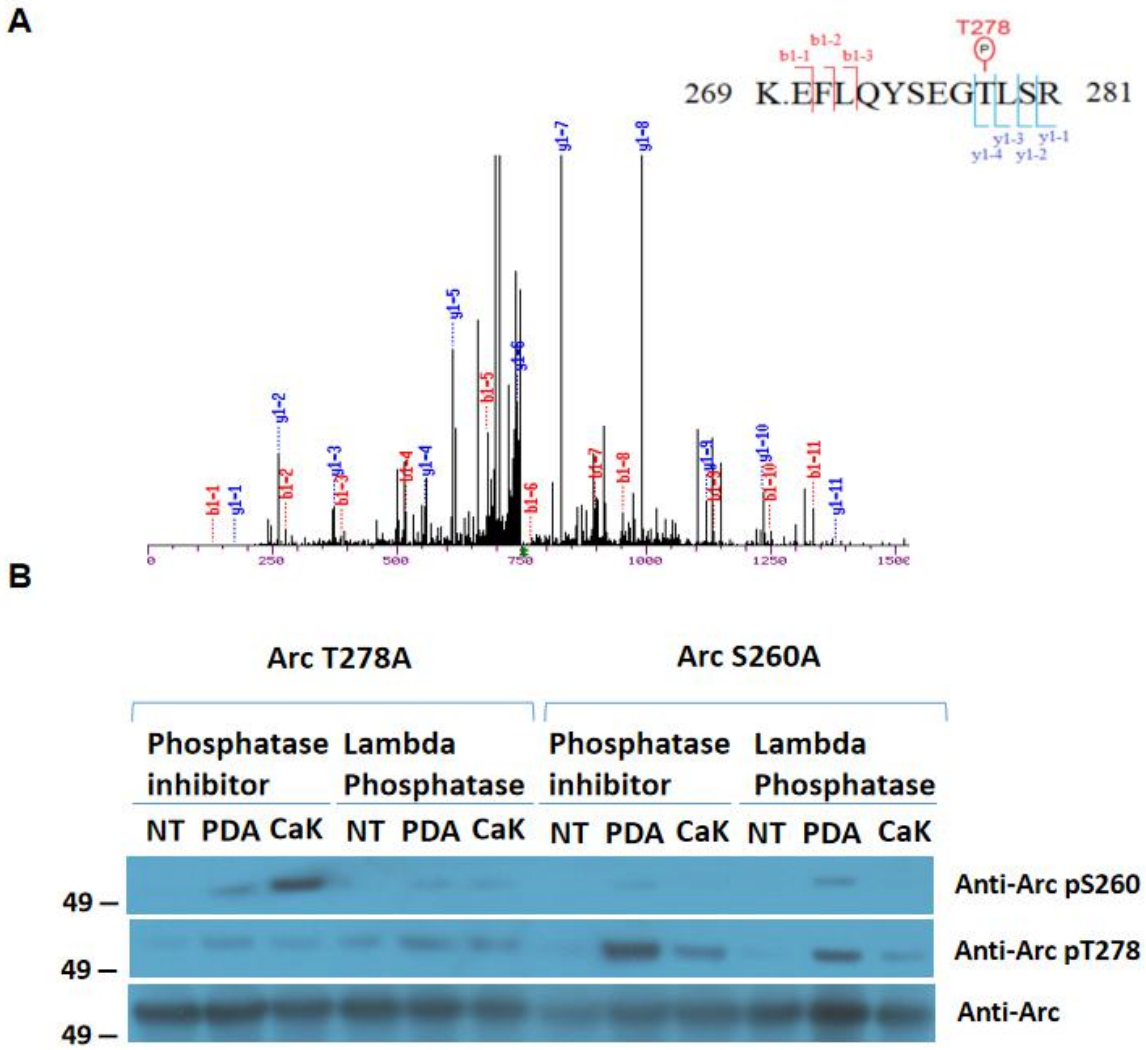

Figure S1, related to Figure 1. Identification of Arc phosphorylation sites. (A) Mass spectrometry profile of Arc. The sequence of Arc from 269-281 is shown. Analysis by MS/MS revealed the presence of phosphorylated modification. The fragment ions whose m / z value corresponds to y or b ions are indicated. The observed fragment ions are labeled on the spectrum and peptide sequence. **(B)** ArcS260A or ArcT278A was co-transfected with or without constitutively active CamKIIα T286D (CaK) to HEK293 cells and treated with or without PDA, and cell lysates were blotted with ArcS260 or ArcT278 phospho-specific antibody. The blot reveals the specific and non-specific reactivity of phospho Abs as well as CaMKII phosphorylation of ArcS260 and PDA-induced phosphorylation of ArcT278.

Figure S2

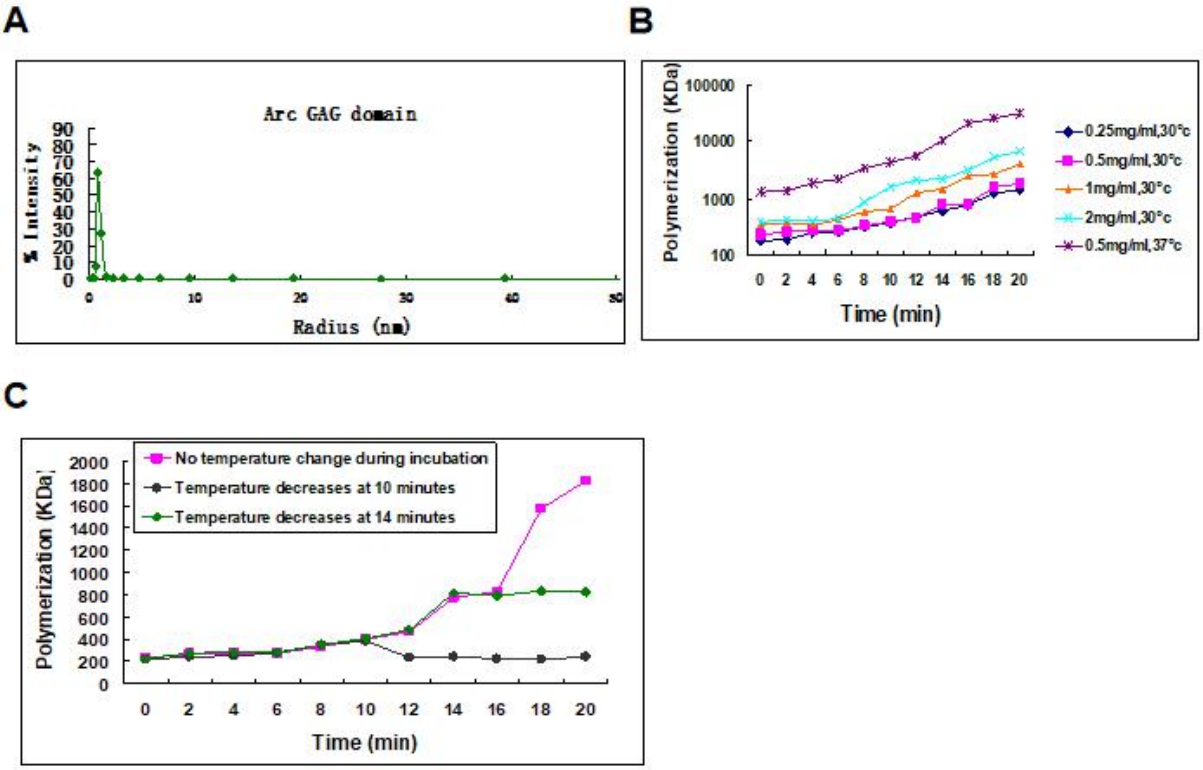
A
Arc GAG domain
% Intensity
Radius (nm)
B
Polymerization (KDa)
Time (min)
0.25mg/ml,30°c
0.5mg/ml,30°c
1mg/ml,30°c
2mg/ml,30°c
0.5mg/ml,37°c
C
Polymerization (KDa)
Time (min)
No temperature change during incubation
Temperature decreases at 10 minutes
Temperature decreases at 14 minutes
D
Arc N-lobe
α1'
Arc C-lobe
E
Arc N-lobe
α1'
Arc C-lobe

Figure S2, related to Figures 3 and 4. Polymerization of Arc. (A) The isolated Arc GAG domain (200μM) examined by DLS remained monomeric at 30°C. **(B)** Monitoring of the oligomeric state of full-length Arc by DLS with varying protein concentration and incubation temperature. The incubation temperature was set to increase from 20°C at 1°C/min. T = 0 indicates when the incubation temperature reached 30°C or 37°C. (**C)** The reversibility of the Arc polymerization process was investigated by monitoring changes of polymerization status while decreasing incubation temperature to 20°C at different time points. The initial concentration of full length Arc is 0.5mg/ml and incubation temperature is 30°C. (**D-E)** Asymmetric oligomerization of Arc N- and C-lobes permits multiple potential modes for full-length Arc polymerization. Hypothetical oligomers created by Arc N-lobe **(D)** and Arc C-lobe **(E)** interactions by application of crystal symmetry to the protomer present in the asymmetric unit mediated with their dimer interfaces (PDB ID, 4X3I and 4X3X). Because interactions are asymmetric individual lobes can potentially mediate extended oligomers. Arc N-lobe polymer is docked on the 1' helix of Arc C-lobe in both **(D)** and **(E)** without its homophilic partner to illustrate the configuration of the full-length Arc molecule. Red lines and purple sheet indicate dimer interface and N-lobe's binding partner, respectively.

Figure S3

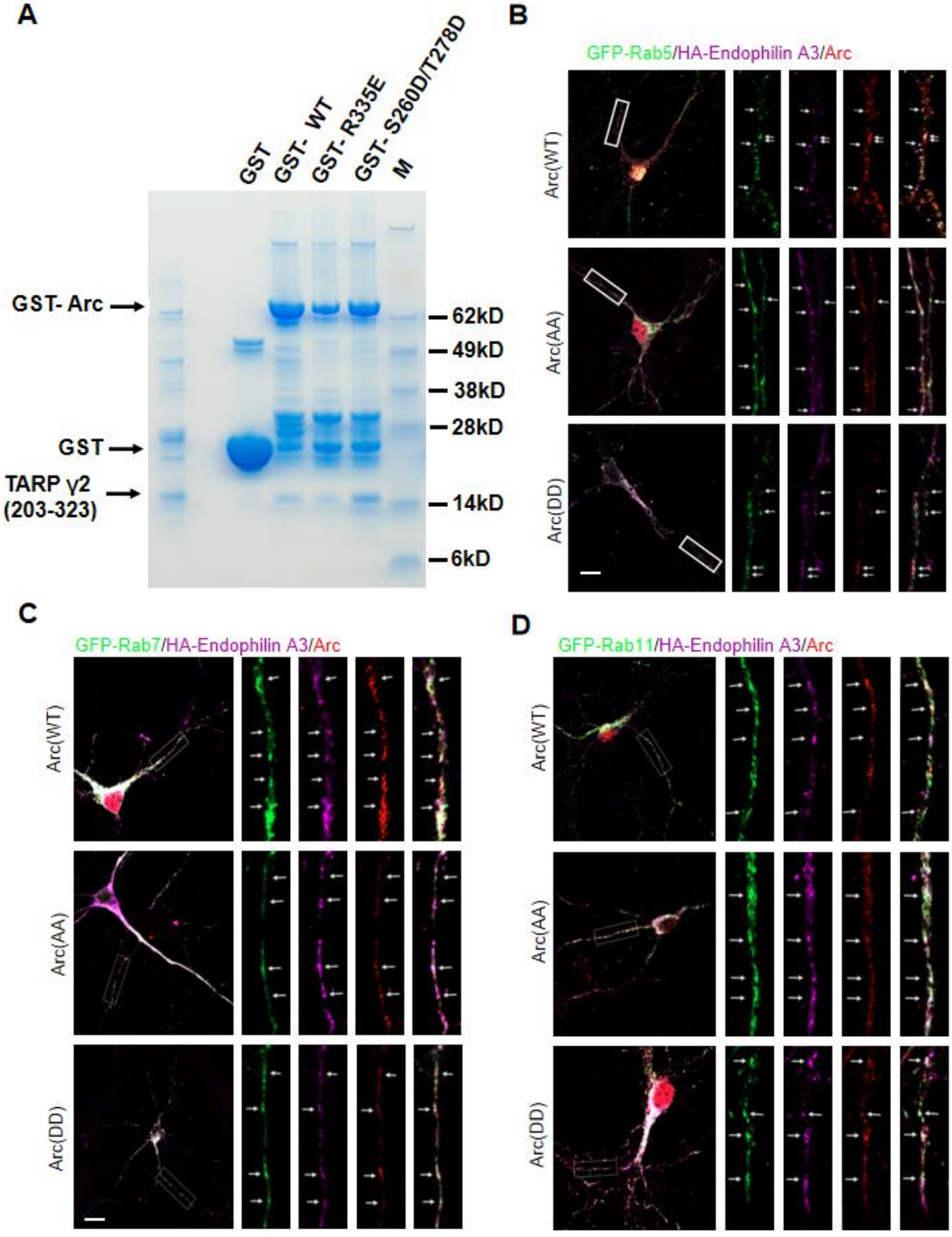
A
GST
GST- WT
GST- R335E
GST- S260D/T278D
M
GST- Arc
GST
TARP γ2
(203-323)
62kD
49kD
38kD
28kD
14kD
6kD
B
GFP-Rab5/HA-Endophilin A3/Arc
Arc(WT)
Arc(AA)
Arc(DD)
C
GFP-Rab7/HA-Endophilin A3/Arc
Arc(WT)
Arc(AA)
Arc(DD)
D
GFP-Rab11/HA-Endophilin A3/Arc
Arc(WT)
Arc(AA)
Arc(DD)

Figure S3, related to Figure 5. Arc mutations that prevent oligomerization do not disrupt N-lobe binding or association with endosomal proteins. (A) Pulldown of TARPγ2 cytoplasmic tail (a.a. 203-323) using GST WT full-length Arc, double phosphomimic mutant ArcS260D/T278D, and Arc C-lobe mutant R335E. (**B, C, D)** Representative images of ArcWT, ArcS260A/T278A (ArcAA) or ArcS260D/T278D (ArcDD) co-localized with endophilin 3 and Rab5, Rab7 and Rab11 transgenes.

Figure S4

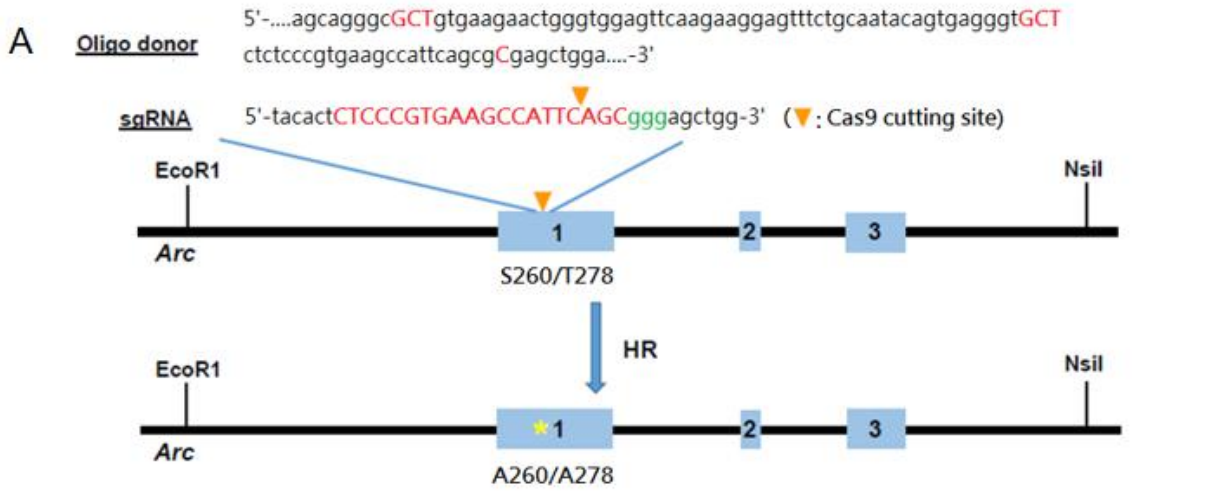
A
Oligo donor
5'-....agcagggcGCTgtgaagaactgggtggagttcaagaaggagtttctgcaatacagtgagggtGCT
ctctcccgtgaagccattcagcgCgagctgga....-3'
sgRNA
5'-tacactCTCCCGTGAAGCCATTCAGCgggagctgg-3' (▼: Cas9 cutting site)
EcoR1
NsiI
Arc
1
2
3
S260/T278
HR
EcoR1
NsiI
Arc
*1
2
3
A260/A278


B
HR

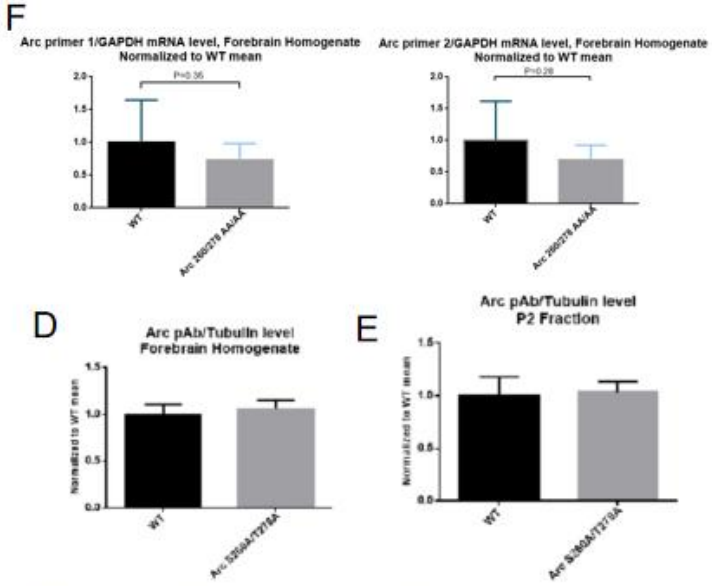
F
Arc primer 1/GAPDH mRNA level, Forebrain Homogenate
Normalized to WT mean
Arc primer 2/GAPDH mRNA level, Forebrain Homogenate
Normalized to WT mean
WT
D
Arc pAb/Tubulin level
Forebrain Homogenate
E
Arc pAb/Tubulin level
P2 Fraction

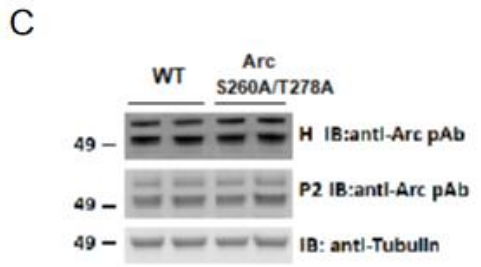
C
WT
Arc
S260A/T278A
49 –
H IB:anti-Arc pAb
P2 IB:anti-Arc pAb
IB: anti-Tubulin

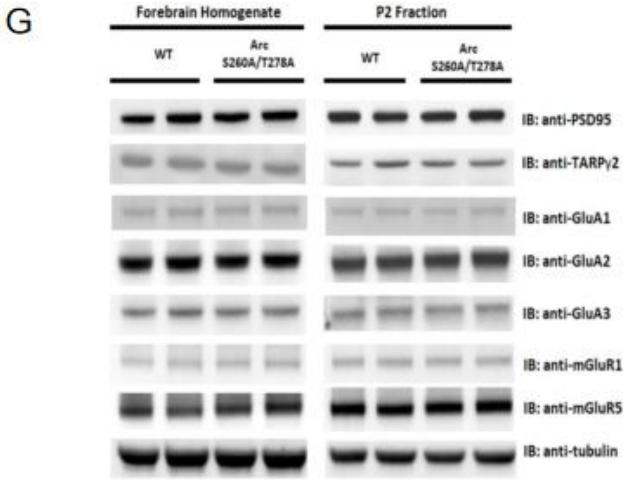
G
Forebrain Homogenate
P2 Fraction
WT
Arc
S260A/T278A
IB: anti-PSD95
IB: anti-TARPγ2
IB: anti-GluA1
IB: anti-GluA2
IB: anti-GluA3
IB: anti-mGluR1
IB: anti-mGluR5
IB: anti-tubulin

Figure S4, related to Figure 6. Arc$^{S260A/T278A}$ KI mouse is generated by CRISPR genome-editing. (A) Design of oligonucleotide template and sgRNA. Three mutations are created to convert serine 260 and threonine 278 of Arc to alanine, as well as to remove a PAM site on the template. (**B)** Genotyping by sequencing shows the precise alterations of *Arc* sequence. (**C)** Representative immunoblotting with anti-Arc polyclonal antibody shows no significant change of basal expression of Arc in forebrain homogenate or P2 fraction lysate between WT and homozygous Arc $^{S260A/T278A}$ KI (Arc 260/278 AA/AA) mice. (**D)** Quantification of (**C)**, the Arc to β-Tubulin level in forebrain, normalized to the mean of WT. n = 6 for each group. (**E)** Quantification of (**C)**, the Arc to β-Tubulin level in P2 fraction, normalized to the mean of WT. n = 6 for each genotype. (**F)** Quantitative PCR of Arc to GAPDH mRNA level in forebrain, normalized to the mean of WT. Two sets of Arc primers were used. n = 6 for each group.
(G) No significant change of representative synaptic proteins in forebrain homogenate or P2 fraction comparing Arc 260/278 AA/AA and littermate WT mice.

Figure S5

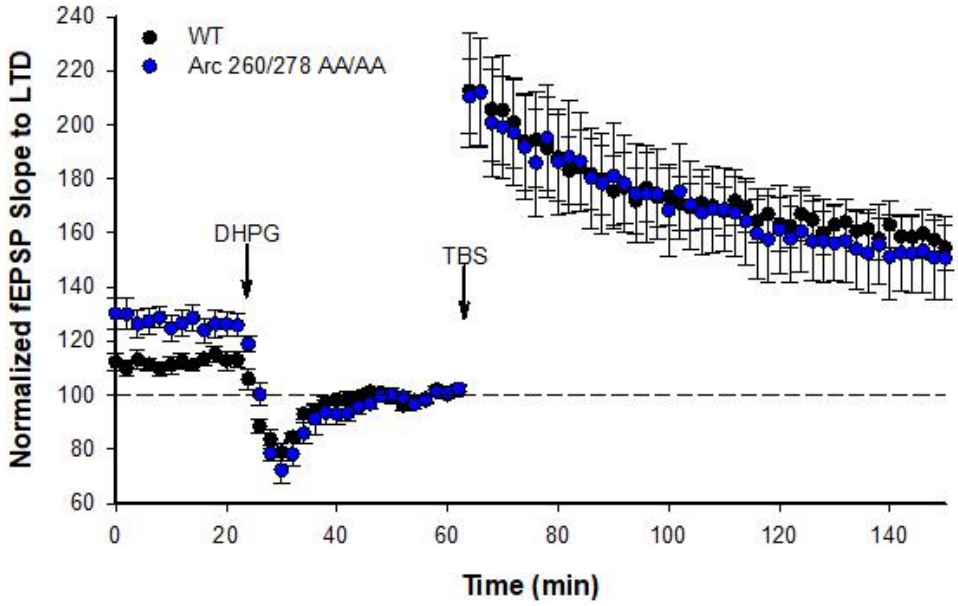

Figure S5, related to Figure 6. TBS-induced LTP following DHPG-LTD is not altered in Arc 260/278 AA/AA mutant mice when normalized to the last 6 min of LTD.

Figure S6

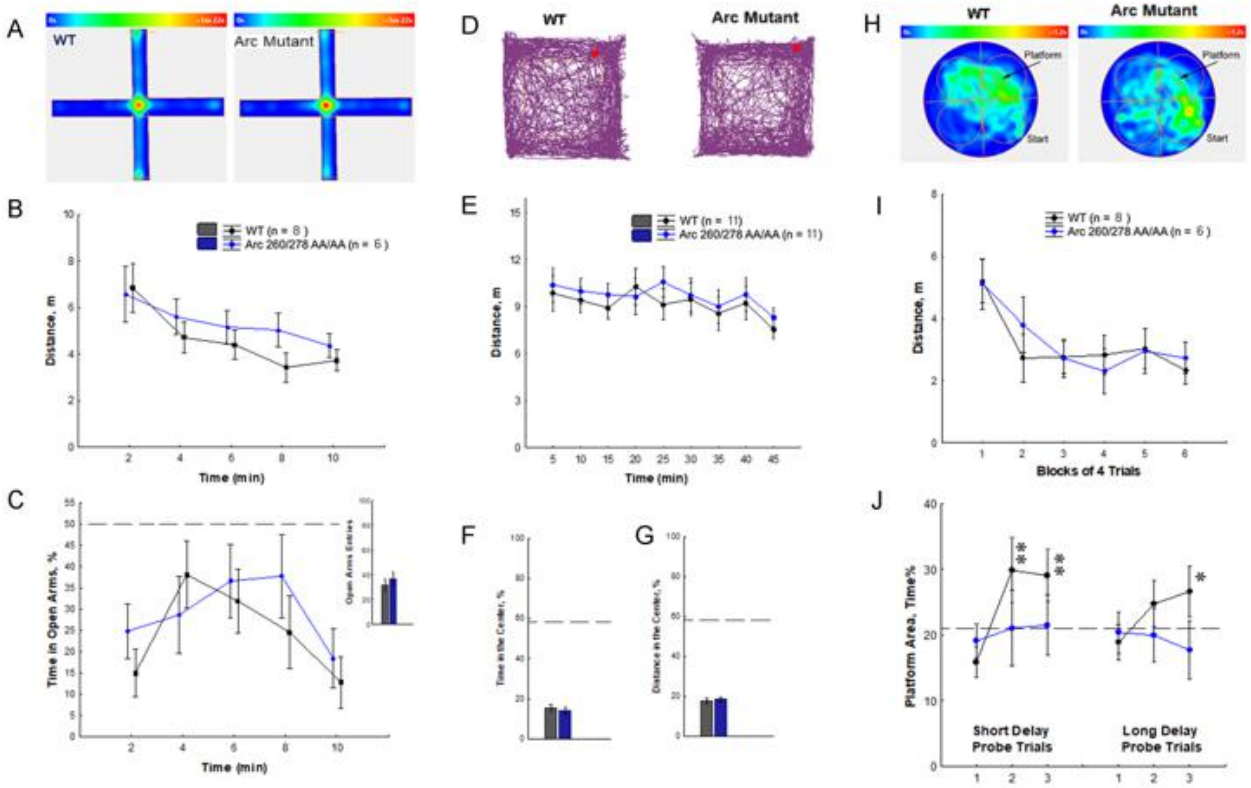

Figure S6, related to Figure 7. Arc 260/278 AA/AA mutant mice show no changes in levels of anxiety or novelty-induced motor activity but have less accurate spatial memory.

(A) Heat maps of the group mean for the animals' position in Plus maze. (**B**) Dynamics of motor activity in Plus maze. No genotype-related differences were detected by a two-way mixed design ANOVA (Genotype x Time; effect of Time $F(4,48)=10.02$, $p<0.6E-5$). (**C**) Time (%) spent in the open arms as a measure of anxiety. No genotype-related differences were detected by a two-way mixed design ANOVA (Genotype x Time; effect of Time $F(4,48)=3.13$, $p<0.023$). (**D**) Representative tracks of motor activity in an Open field arena. (**E**) Dynamics of exploratory activity in Open field. No genotype-related differences were detected by a two-way mixed design ANOVA (Genotype x Time; effect of Time $F(8,160)=2.19$, $p<0.031$). (**F**) Time (%) spent in the central area of the open field as a measure of anxiety. No genotype-related differences were

detected (one-way ANOVA, $p>0.65$). (**G**) Distance (%) travelled through the central area as a measure of anxiety. No genotype-related differences were detected (one-way ANOVA, $p>0.72$). Dotted lines in (**C, F - G)** indicate chance levels based on the relative size of anxiogenic areas in the Plus maze **(C)** and Open field **(F-G)**. Note that both Plus maze and Open field are potent at inducing anxiety-related avoidance behaviors. (**H)** Heat maps of the group means for the animals' position in Morris water maze. (**I)** Dynamics of distance swam to the platform. No genotype-related differences were detected by a two-way mixed design ANOVA (Genotype x Time). Significant effect of Trial Block (ANOVA, $F(5, 60)=4.73$, $p<0.001$, no significant interaction) indicated that both genotypes improved their performance during training. (**J)** Spatial preference (Time%) to an Area around the platform. The Platform Area was fitted to the quadrant around the platform as shown in (**H)**. A chance level of preference to the Platform Area is shown by a dotted line (21%). Spatial memory was tested in probe trials with short (30 min) and long delays (20 hrs) after the last training trial of each training day (days 1,2,3). Only WT controls demonstrated performance with spatial preferences above the chance level. Double and single asterisks indicate significant differences from the chance level: $p<0.005$ and $p<0.01$, respectively (two-sided t-test). However, differences in spatial preferences between genotypes did not reach significance in this cohort (two-way ANOVA, $p>0.05$). Note, that in contrast to spatial memory tested in the MWM, Arc 260/278 AA/AA mutant mice revealed significant deficits in the acquisition of contextual fear memory (Figure 7). These findings suggest that the effects of Arc 260/278 AA/AA mutation on cognitive phenotypes are the strongest in a setting that involves a fast acquisition of information.

Figure S7

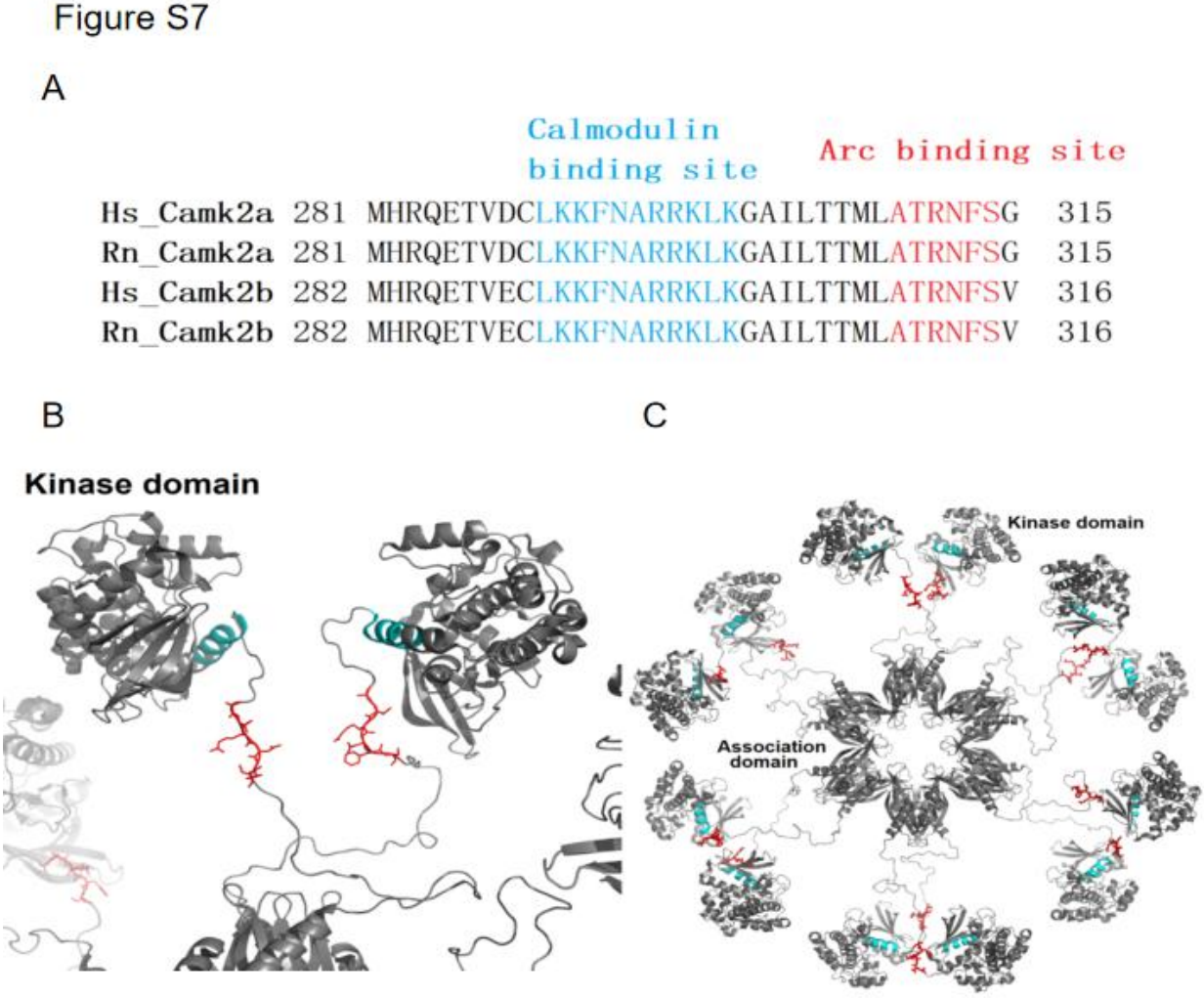

Figure S7, related to Figure 2. Conservation and physical proximity of Arc binding site to Calmodulin binding site in CaMKIIα and CaMKIIβ. (A) Sequence alignment of the regulatory region in CaMKIIα and CaMKIIβ from two typical species. Hs_ CaMKIIα, NP_057065; Rn_ CaMKIIα, NP_037052; Hs_ CaMKIIβ, NP_001211; Rn_ CaMKIIβ, NP_001035813. Calmodulin binding site and Arc binding site are shown in blue and red, respectively. **(B, C)** Stick representation of the CaMKIIα holoenzyme (PDB ID, 5U6Y). Calmodulin binding site is displayed in blue, and Arc binding site is in red. Note that the Arc binding site in the linker domain is unstructured and accessible for binding in the inactive holoenzyme.